MECSOL 2022 - Proceedings of the 8th International Symposium on Solid Mechanics
M.L. Bittencourt, J. Labaki, L.C.M. Vieira Jr. and E. Mesquita (Editors), Campinas SP, Brazil, October 17th to 19th, 2022

Non-watertight geometries and boundary element models

Gustavo de Oliveira Daumas 1, Rafael Marques Lins 1, Sérgio Gustavo Ferreira Cordeiro 1, Francisco Alex Correia Monteiro 1

[1] Technological Institute of Aeronautics, Laboratory of Structural Modelling, Praça Marechal Eduardo Gomes, 50, 12228-900. São José dos Campos-SP, Brazil

Abstract: It is well known that the boundary integral equations of linear elasticity are exact mathematical representations of the governing differential equations when the integrals are written over closed surfaces (or closed curves in plane problems). However, practical geometrical design technics (namely, NURBS curves and surfaces) often do not render a perfectly watertight boundary representation of the domain. Thus, non-watertight boundary geometries with small gaps are often generated. In the present study, one investigates how such unsought gaps affect the response of boundary elements models. The obtained results have pointed out that, as long as the gaps are small enough, non-watertight boundary geometries may produce valuable solutions for practical purposes.

Keywords: boundary integral equations, non-watertight boundary geometries, boundary elements models

INTRODUCTION

Stress analyses of mechanical components used for various purposes are of vital importance to ensure the structural safety of the original geometrical design of the component. To improve safety, engineers spend a significant amount of time in the design, modeling, and analysis of each component. The geometrical design models of the mechanical components are first developed by designers in computer-aided design (CAD) software. Then, numerical methods, such as the finite and boundary element methods (Zienkiewicz and Taylor, 1967; Brebbia and Dominguez, 1989) are employed to perform the stress analysis. Before the analysis, a suitable model for the analysis must be provided from the geometrical CAD models. The most common geometrical models are built as a set of independent parametric curves (for 2D geometries) or surfaces (for 3D geometries), which describes the boundary of the solid. Such models are known in the literature as Boundary-representation (B-representation) models (Sederberg and Parry, 1986). Usually, the B-representation models must be converted into suitable finite element models. This involves several intermediate steps (Ray et al., 2014). The first step is to obtain a B-representation without gaps in the intersections of the independent curves or surfaces. The last step is to generate a standard volumetric finite element mesh for analysis purposes. Problems often arise in ensuring no gaps in the curves or surfaces intersections. With the standard CAD technologies, namely Non-Uniform Rational B-splines (NURBS) curves and surfaces (Piegl and Tiller, 1995; Roger, 2001), small gaps are generally inevitable (Sederberg et al., 2003, Bazilevs et al. 2010). When small gaps exist in a B-representation model, it is called a non-watertight geometrical model. Non-watertight models are usually avoided in the design through analysis process, since for the standard analysis technology, namely the finite element method (Zienkiewicz and Taylor, 1967) and other domain and meshless methods (Belytschko, 1994; Strouboulis et al, 2001), the existence of gaps impossibilities the standard volumetric mesh (or regularly distributed internal points) generation. This issue is by far a nontrivial task for geometric complex engineering designs, as pointed out by Cottrell et al. (2009). The conversion of geometrical models to suitable analysis models has been studied by Ted Blacker, Manager of Simulation Sciences, Sandia National Laboratories. and usually takes 80% of the hole design-through analysis process time (Cottrell et al., 2009). Linear differential equations governing a given boundary value problem can be rewritten as boundary integral equations when the fundamental solution is known (Brebbia and Dominguez, 1989). The boundary integral equations of linear elasticity are well-stablished nowadays and can be properly solved by the Boundary Element Method (BEM) (Brebbia and Dominquez, 1989; Aliabadi, 2002). The main characteristic of BEM is that, since it was developed to solve boundary integral equations, domain meshes are avoided, and the parametrizations are required only at the boundaries of the solids. This feature makes the construction of BEM models from CAD geometries largely attractive because both CAD and BEM are based on the B-representation of the solids. The construction of BEM models from CAD geometries for numerical analysis purposes has been reported in several works in the literature (Simpson et al., 2012, Simpson et al., 2013, Lian, et al., 2013; Scott et al., 2013). The boundary integral equations are exact mathematical representations of the problem if they are written over watertight (closed) boundaries. If only a non-watertight B-representation is available, the boundary integral equations are, in the best case, only approximately true. Since integrals can be understood as summation, the contributions that will not appear in the integral equations due to the missing areas in gaps will introduce errors in the previously mathematically exact boundary integral equations.

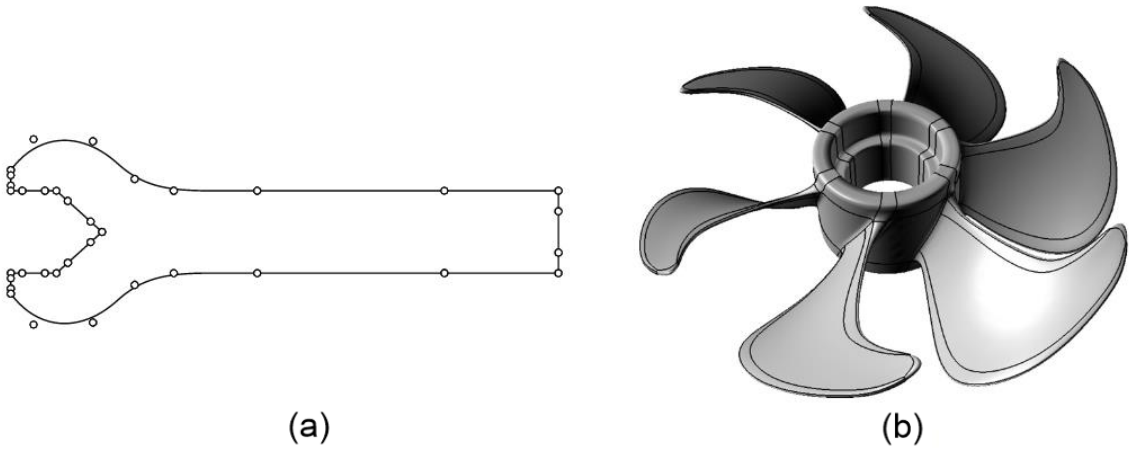

Figure 1 – Geometrical B-representation models: a) 2D model (Simpson et al., 2012). b) 3D model (Scott et al., 2013)

In the present work, one claims that if the gaps of the non-watertight B-representations are small enough, such errors will be small enough and the boundary integral equations written over the non-watertight boundaries can still be solved by the BEM. The discontinuous boundary elements presented in Aliabadi (2002) are employed in the analysis in order to be able to study problems with very small gaps without generating almost singular systems of equations due to very close colocation points. A convergence study in terms of the total external work and other local quantities (displacements and stresses) is performed in two examples.

BOUNDARY-REPRESENTATION GEOMETRICAL MODELS

The B-representation geometrical models assume that the boundary $\boldsymbol{\Gamma}$ of a given domain can be described by the union of a set of independent curves $\boldsymbol{C}_i$ (for 2D geometries) or surfaces $\boldsymbol{S}_i$ (for 3D geometries):

$$\boldsymbol{\Gamma} = \{\boldsymbol{C}_i\} \text{ or } \boldsymbol{\Gamma} = \{\boldsymbol{S}_i\} \tag{1}$$

Figure 1a illustrates a B-representation 2D geometrical model of a spanner while Fig. 1b illustrates a B-representation 3D geometrical model of a propeller.

In general, the boundary of a geometrical object cannot be fully described by a set of standard CAD curves and surfaces technologies, namely B-splines and NURBS. Gaps in the curves and surfaces intersections may be observed for B-representations of topologically complex objects (Marussig and Hugues, 2018). For these models, i.e., Non-watertight B-representations, the union of the parametric curves or surfaces is just an approximation $\tilde{\boldsymbol{\Gamma}}$ of the "real" boundary $\boldsymbol{\Gamma}$:

$$\boldsymbol{\Gamma} = \tilde{\boldsymbol{\Gamma}} \cup \boldsymbol{\Gamma}_g \tag{2}$$

where $\boldsymbol{\Gamma}_g$ are missing boundaries due to gap0s. Even though CAD technologies such as B-splines and NURBS surfaces are the standard CAD technologies and represent billions of dollars in investment, Non-watertight NURBS based B-representations are inevitable in general CAD geometrical modeling, thus limiting the analysis once FEM analysis suitable mesh generation requires watertight geometrical models (Bazilevs et al., 2010).

THE BOUNDARY ELEMENT METHOD

The boundary element method (BEM) is a widely used method for solving linear elastostatic problems. The method is based on the Boundary Integral Equations (BIE) of the governing problem, which can be obtained from the weighted integral form of the differential equations of the boundary value problem by using the fundamental solution (Brebbia and Dominguez, 1989). Once all domain integrals are transformed into boundary integrals, the problem can be treated with one lower dimension discretization compared to domain discretization methods.

Boundary integral equations of linear elasticity

The mechanical response of a given linear elastic solid with domain $\boldsymbol{\Omega}$ and boundary $\boldsymbol{\Gamma}$, such as the one illustrated in Fig. 2, can be represented in terms of the BIEs. The boundary can be decomposed into two parts $\boldsymbol{\Gamma} = \boldsymbol{\Gamma}_\mathrm{u} \cup \boldsymbol{\Gamma}_\mathrm{t}$, where $\boldsymbol{\Gamma}_\mathrm{u}$ is the part where geometrical boundary conditions are prescribed, i.e., the displacement is known, and $\boldsymbol{\Gamma}_t$ is the part where natural boundary conditions are prescribed, i.e., the tractions are known.

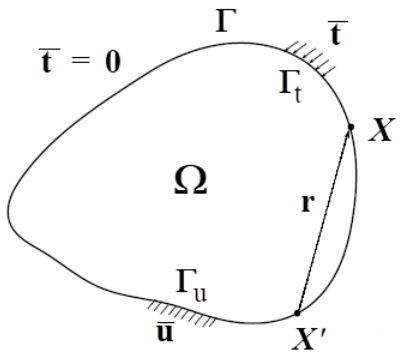

Figure 2 – Problem and boundary collocation point definition

The displacement BIE, assuming the body forces as nil, is written as follows:

$$c_{ij}(\mathbf{X}')u_j(\mathbf{X}') = \int_{\mathbf{\Gamma}} U_{ij}(\mathbf{X}',\mathbf{X})t_j(\mathbf{X})\,\mathrm{d}\mathbf{\Gamma} - \mathcal{C}\int_{\mathbf{\Gamma}} T_{ij}(\mathbf{X}',\mathbf{X})u_j(\mathbf{X})\,\mathrm{d}\mathbf{\Gamma} \tag{3}$$

where $\mathbf{X}'$ and $\mathbf{X}$ indicates the source and field points, respectively. $u_j(\mathbf{X}')$ is the displacement at $\mathbf{X}'$. $u_j(\mathbf{X})$ and $t_j(\mathbf{X})$ are boundary displacements and tractions and, $U_{ij}(\mathbf{X}',\mathbf{X})$, $T_{ij}(\mathbf{X}',\mathbf{X})$ are, respectively, the Kelvin fundamental solutions for displacements and tractions, which are functions of the distance $r = \|\mathbf{r}\| = \|\mathbf{X} - \mathbf{X}'\|$ (Aliabadi, 2002). $\mathcal{C}\int$ indicates that the integral is evaluated in the Cauchy Principal Value sense and $c_{ij}(\mathbf{X}')u_j(\mathbf{X}')$ is the free term arising from the singular integral. For a non-watertight boundary $\tilde{\mathbf{\Gamma}}$, the BIE is not an exact mathematical representation of the problem. However

$$c(\mathbf{X}')u_i(\mathbf{X}') \approx \int_{\tilde{\mathbf{\Gamma}}} U_{ij}(\mathbf{X}',\mathbf{X})t_j(\mathbf{X})\,\mathrm{d}\tilde{\mathbf{\Gamma}} - \mathcal{C}\int_{\tilde{\mathbf{\Gamma}}} T_{ij}(\mathbf{X}',\mathbf{X})u_j(\mathbf{X})\,\mathrm{d}\tilde{\mathbf{\Gamma}} \tag{4}$$

as long as the missing gap boundaries $\mathbf{\Gamma}_g$ are small enough compared to $\mathbf{\Gamma}$, i.e., $\|\mathbf{\Gamma}_g\| \ll \|\mathbf{\Gamma}\|$.

Continuous and discontinuous boundary elements

Approximations are required for obtaining numerical solutions from the collocation of the previous presented BIE´s. Assuming the errors in the BIE (4) as negligible, an equality condition can be accepted and thus, only the boundary $\tilde{\mathbf{\Gamma}}$ must be discretized into boundary elements, over which displacements, tractions, and the boundary geometry are approximated. Then,

$$c_{ij}(\mathbf{X}')u_j(\mathbf{X}') + \sum_{e=1}^{\mathrm{NE}}\int_{\mathbf{\Gamma}_e} T_{ij}\big(\mathbf{X}',\mathbf{X}(\xi)\big)N^{\alpha}(\xi)J(\xi)d\xi u_j^{\alpha} = \sum_{e=1}^{\mathrm{NE}}\int_{\mathbf{\Gamma}_e} U_{ij}\big(\mathbf{X}',\mathbf{X}(\xi)\big)N^{\alpha}(\xi)J(\xi)d\xi t_j^{\alpha} \tag{5}$$

where NE indicates the number of boundary elements utilized for discretizing the boundary $\tilde{\mathbf{\Gamma}}$, $\mathbf{\Gamma}_e$ represents the parametric curve or surface of a given element e, $N^{\alpha}(\xi)$ are basis functions (Lagrange polynomials are adopted in the present work), $J(\xi)$ is the Jacobian of the parametric element mapping and u_j^{α} and t_j^{α} are the displacements and tractions components at the collocation points, respectively. The singular integrals in (5) are treated by the subtraction singularity technique (Aliabadi, 2002) and the remaining regular integrals are performed with standard Gaussian quadrature. The BEM usual system of equations is thus obtained from the collocation of (5) at all boundary collocation points. Discontinuous boundary elements, such as those presented in Aliabadi (2002) and illustrated in Fig. 3, are also adopted to discretize $\tilde{\mathbf{\Gamma}}$.

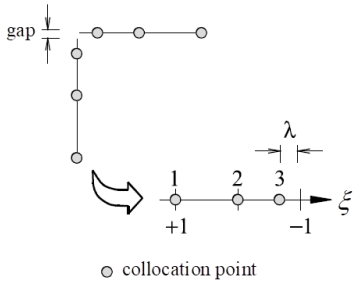

Figure 3 – Discontinuous boundary elements (Aliabadi, 2002 - adapted)

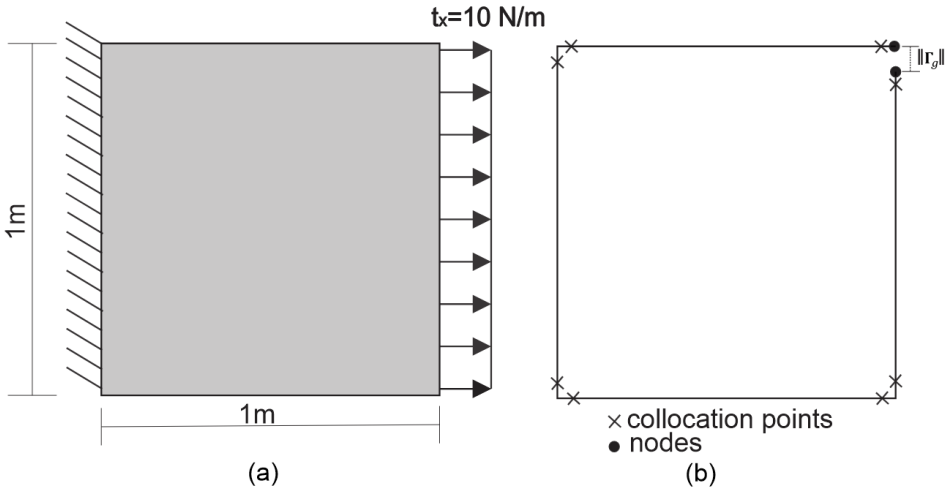

Figure 4 – Tensile sheet: (a) problem definition (b) boundary element mesh

Discontinuous elements are employed to solve the discontinuous tractions fields' problems, as usual in BEM analysis. However, they are also adopted in the present work to avoid collocation points extremely close to each other near the small gaps of the B-representation (see Fig. 3). Thus, it is possible to ensure that the BEM system of equations will not be numerically singular for non-watertight models with very small gaps.

NUMERICAL RESULTS

The sensibility of BEM results with respect to the gap size in non-watertight boundary element models was verified through two examples: 1) a tensile sheet and 2) a tensile sheet with a circular hole. The sensibilities of the numerical results were evaluated with respect to the analytical and the numerical reference responses, for the first and the second examples, respectively. The singular integrals were regularized by the subtraction singularity technique and all numerical integrals were evaluated with standard Gauss quadrature. A convergence test proved that 8 integration points is enough to provide accurate results for the presented examples. 900 Gauss points were also adopted for the integrations, in order to demonstrate that the errors are induced manly due to the gaps.

Tensile sheet

The first example is a linear elastic tensile square sheet. The dimensions and boundary conditions of the problem are illustrated in Fig. 4a. Figure 4b illustrates the boundary mesh, composed of 4 linear elements (8 collocation points). The adopted material properties were a Young´s modulus $E = 100\ \mathrm{N/m^2}$ and a Poisson's ratio $\nu = 0$. Since the analytical displacement and traction boundary fields of this problem are known, the exact external work result $W_{ex} = \int_{\boldsymbol{\Gamma}} \mathbf{u} \cdot \mathbf{t}\, d\boldsymbol{\Gamma} = 1.0\ \mathrm{Nm/m}$. The sensitivity analyses are carried out based on the numerical values of the external work obtained from the BEM models: $W = \int_{\tilde{\boldsymbol{\Gamma}}} \tilde{\mathbf{u}} \cdot \tilde{\mathbf{t}}\, d\tilde{\boldsymbol{\Gamma}}$, in which $\tilde{\mathbf{u}}$ and $\tilde{\mathbf{t}}$ are boundary approximations for displacements and tractions, and $\tilde{\boldsymbol{\Gamma}}$ is defined by the union of the boundary elements. For the watertight BEM model, i.e., $\|\boldsymbol{\Gamma}_g\| = 0$, $\tilde{\boldsymbol{\Gamma}} = \boldsymbol{\Gamma}$ and the ratio W/W_{ex} is expected to be very close to 1.0. In fact, the error in the numerical external work w for this case was close to $1.0\mathrm{E}-14$, which is the same order of magnitude of the machine precision. On the other hand, for non-watertight BEM models, the ratio W/W_{ex} is expected to deviate from the unity as $\|\boldsymbol{\Gamma}_g\|$ deviates from zero.

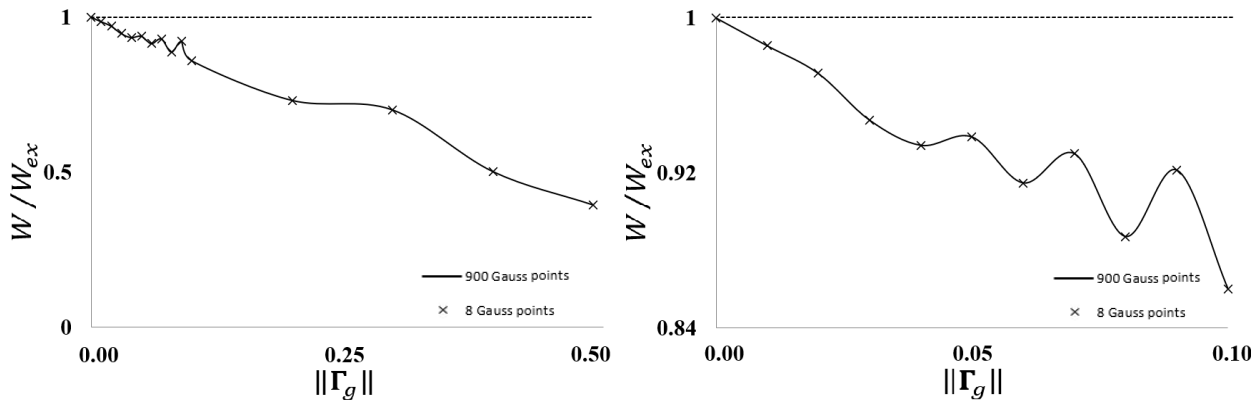

Figure 5 – Ratio of external work versus gap size

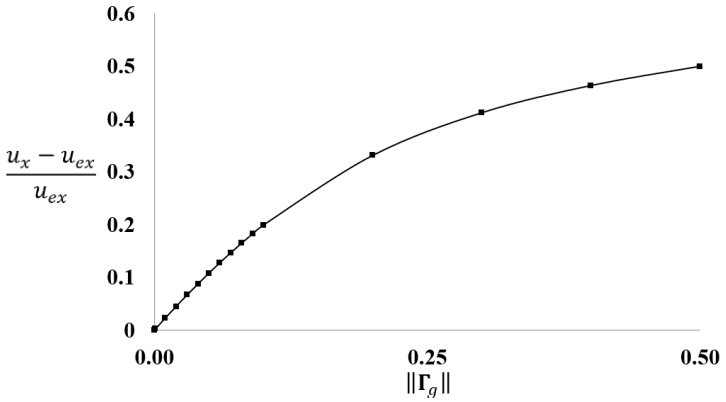

Figure 6 – Relative displacement error versus gap size

The ratio W/W_{ex} responses obtained from BEM models with $\|\Gamma_g\|$ ranging from 0.0 to 0.5 are shown in Fig. 5 (left). Figure 5 (right) shows a zoom of Fig. 5 (left) for $\|\Gamma_g\|$ ranging from 0.0 to 0.1. It is interesting to point out that the gap, deliberately inserted with sizes ranging from 0.025% to 12.5% of the hole boundary size, introduced errors in the external work W ranging from 1.044% to 60.7%. Thus, the errors for global energy quantities are negligible only for very small gaps. Figure 6 illustrates the relative error for local quantities, such as the horizontal displacement of the collocation point in the vertical edge that is the closest to the gap. Notice that, knowing the exact solution $u_{ex} = 0.1$ m for the horizontal displacement, it is possible to observe that the gap introduced relative errors in u_x ranging from 0.23% to 50.0%.

Tensile sheet with a circular hole

The second example is a linear elastic tensile sheet with a circular hole. The dimensions and boundary conditions of the problem are illustrated in Fig. 7a. Figure 7b illustrates the boundary mesh, composed of 80 elements (116 collocation points). The adopted material properties were the same of the previous example. The sensibility in the stress response at the points A and B of the hole (see Fig. 7a) due to the deliberately inserted gap was studied. For the watertight BEM model, i.e. $\|\Gamma_g\| = 0$, the value obtained for σ_x in both points was $\sigma_{ref} = 35.6978$ MPa. The ratios σ_A/σ_{ref} and σ_B/σ_{ref} obtained from the non-watertight BEM models with $\|\Gamma_g\|$ ranging from 0.0 to 0.5 are shown in Fig. 8 (left), where σ_A and σ_B stands for the σ_x stress component at points A and B, respectively. Figure 8 (right) shows a zoom of Fig. 8(left) for $\|\Gamma_g\|$ ranging from 0.0 to 0.1.

The results showed that the gap, deliberately inserted with sizes ranging from 0.025% to 12.5% of the hole boundary size, introduced errors in the σ_x values ranging from 0.052% to 41.5%. Thus, it can be concluded that the errors in the stresses can be neglected only for very small gaps. Notice also that the introduction of the gap makes the structural response present a spurious asymmetry, which can be observed in the different values assumed for the stresses σ_A and σ_B.

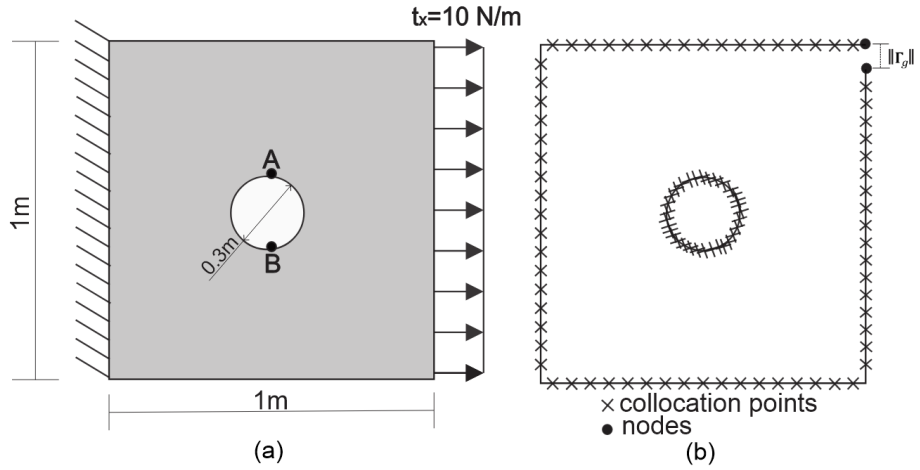

Figure 7 – Tensile sheet with a circular hole

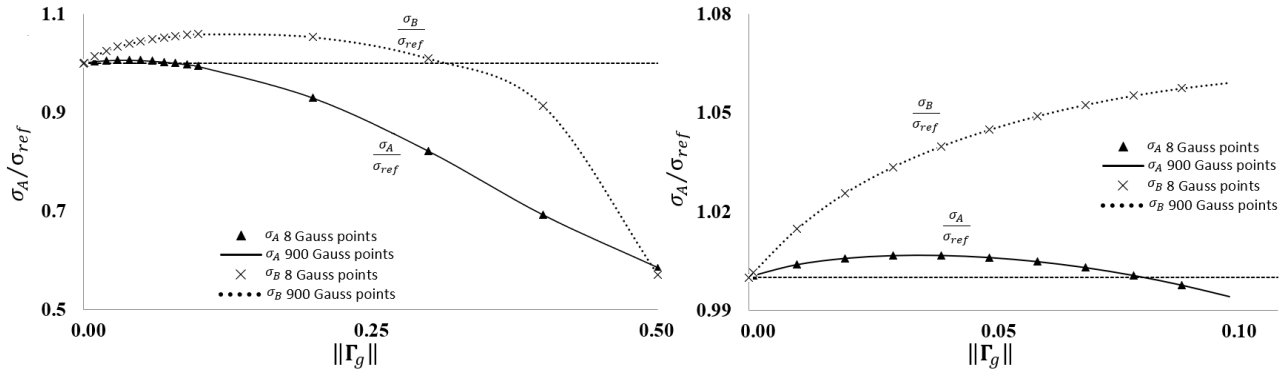

Figure 8 – Relative stress versus gap size

CONCLUSION

The present study investigated the sensitivity of BEM numerical responses in terms of global (external work) and local (displacements and stresses) quantities with respect to the size $\|\boldsymbol{\Gamma}_g\|$ of the unsought gaps in non-watertight models. Adopting discontinuous elements, it is possible to ensure that collocation points very close to each other will not appear in the near small gap's boundaries. Thus, a near singular system of equations is avoided. The obtained results have pointed out that, as long as the gaps are small enough, non-watertight boundary geometries may produce valuable solutions for practical purposes. Since the surface interception gaps inherent to practical geometrical design technics (namely, NURBS curves and surfaces) are usually very small, and are unlikely to reach 2.5% of $\|\boldsymbol{\Gamma}\|$, one can adopt the BEM as a plausible choice for the structural analyses, avoiding the need to redesign the solid in CAD software. Future investigations may include 3D isogeometric elastostatic sensitivity analysis of non-watertight models.

ACKNOWLEDGMENTS

The authors would like to thank the financial support provided by the Coordination for the Improvement of Higher Education Personnel (CAPES).

REFERENCES

Aliabadi, M.H. 2002, "The Boundary Element Method, volume 2: Applications in solids and structures", John Wiley & Sons, Chichester, 592 p.

Bazilevs, Y., Calo, V.M., Cottrell, J.A., Evans, J.A., Hugues, T.J.R., Lipton, S., Scott, M.A., Sederberg, T.W. 2010, "Isogeometric analysis using T-splines", Computer Methods in Applied Mechanics and Engineering, Vol.199, pp. 229-263.

Belytschko, T., Lu, Y.Y., Gu, L. 1994, "Element-free Galerkin methods", International Journal for Numerical Methods in Engineering, Vol.37, pp. 229-256.

Brebbia, C.A., Dominguez, J. 1989, "Boundary Elements: An introductory Course", McGraw Hill, Southampton, 286 p.

Cottrell, A.J., Hughes, T.J.R., Bazilevs, Y. 2009, "Isogeometric Analysis: Toward Integration of CAD and FEA", John Wiley & Sons, Chichester, 355 p.

Lian, H., Simpson, R.N., Bordas, S.P.A. 2013, "Stress analysis without meshing: isogeometric boundary element method", Proceedings of the institution of civil engineers: Engineering and computational mechanics, Vol.166, pp. 88-99.

Marussing, B., Hugues, T.J.R. 2018, "A review of trimming in isogeometric analysis: challenges, data exchange and simulation aspects", Archives of Computational Methods in Engineering, Vol.25(4), pp. 1059-1127.

Peng, X., Arroshchenko, E., Kerfriden, P., Bordas, S.P.A. 2017, "Linear elastic fracture simulation directly from CAD: 2D NURBS-based implementation and role of tip enrichment", International Journal of Fracture, Vol.204, pp. 55-78.

Piegl, L., Tiller, W. 1995, "The NURBS book", Springer, Berlin, 649 p.

Ray, N., Delaney, T., Einstein, D.R., Jiao, X. 2014, "Surface remeshing with robust high-order reconstruction", Eng Comput, Vol.30, pp. 487-502.

Roger, D.F. 2001, "An introduction to NURBS with historical perspective", Morgan Kaufmann Publishers, Burlington, 343 p.

Scott, M.A., Simpson, R.N., Evans, J.A., Lipton, S., Bordas, S.P.A., Hugues, T.J.R., Sederberg, T.W. 2013, "Isogeometric boundary element analysis using unstructured T-splines", Computer Methods in Applied Mechanics and Engineering, Vol.254, pp. 197-221.

Sederberg, T.W., Parry, S.R. 1986, "Free-form deformation of solid geometric models", ACM SIGGRAPH Comput Graphics, Vol.20, pp. 151-160.

Sederberg, T.W, Zheng, J., Bakenov, A., Nasri, A. 2003, "T-splines and T-NURCCs", ACM Transaction on Graphics, Vol.22, pp. 477-484.

Simpson, R.N., Bordas, S.P.A., Trevelyan, J., Rabczuk, T. 2012, "A two-dimensional isogeometric boundary element method for elastostatic analysis", Computer Methods in Applied Mechanics and Engineering, Vol.209, pp. 87-100.

Simpson, R.N., Bordas, S.P.A., Haojie, L., Trevelyan, J. 2013, "An isogeometric boundary element method for elastostatic analysis: 2D implementation aspects", Computers & Structures, Vol.118, pp. 2-12.

Strouboulis, T., Copps, K., Babuška, I. 2001, "The generalized finite element method", Computer Methods in Applied Mechanics and Engineering, Vol.190, pp. 4081-4193.

Zienkiewicz, O.C., Taylor, R.L. 1967, "The finite element method: solid mechanics", Butterworth-heinemann, Oxônia, 221 p.

RESPONSIBILITY NOTICE

The author(s) is (are) the only party(ies) responsible for the printed material included in this paper.